

# THE INFLUENCE OF EL NIÑO AND LA NIÑA EPISODES ON THE FREQUENCY OF EXTREME PRECIPITATION EVENTS IN SOUTHERN BRAZIL

Ieda Pscheidt<sup>1</sup>

Universidade de São Paulo, São Paulo, São Paulo

Alice Marlene Grimm<sup>2</sup>

Universidade Federal do Paraná, Curitiba, Paraná

## 1. INTRODUCTION

The strong and complex ocean-atmosphere coupling in the Pacific Ocean called El Niño-Southern Oscillation (ENSO) causes global impacts, being the strongest climatic signal after the annual cycle. (Enfield e Mestas-Núñez, 1999). ENSO produces sea surface temperature (SST) anomalies and perturbs the global atmospheric circulation, especially the Hadley and Walker circulation (Kidson, 1975; Kousky et. al., 1984; Souza e Ambrizzi, 2002).

Grimm et. al. (2000) verified that southeastern South America (SA), including southern Brazil, Argentina, Chile, Uruguay and Paraguay, is the extratropical region most affected by the extreme phases of ENSO: El Niño (EN) and La Niña (LN) episodes. They reported that the impact of these events on the precipitation in this region is strongest in austral spring of the onset year of the events (year 0). Similar conclusions are found in Mason e Goddard (2001). Grimm et. al. (1998, 2000) also found precipitation anomalies in southern Brazil associated with EN events in the winter of the year after the onset of the episodes (year +).

This paper aims to analyze the impact of EN and LN events on the frequency of extreme precipitation events in Southern Brazil in November (0) and July (+). Besides, the atmospheric conditions associated with extreme events during EN, LN and neutral years are analyzed.

## 2. DATA AND METHODS

Daily precipitation data in the period 1950-2000 from more than 4000 stations from the Brazilian states Rio Grande do Sul, Santa Catarina, Paraná, São Paulo and Mato Grosso do Sul, and from the neighbor countries Argentina, Paraguay and Uruguay were used in this analysis. The data are mostly from the Brazilian Agência Nacional de Águas (ANA) and from the meteorological services of the other countries. Also daily data of sea level pressure, geopotential height, wind and temperature, and specific humidity from the NCEP/NCAR Reanalysis (Kalnay et al., 1996) were used. SST data are from the HadISST data set (Rayner et al. 2003)

1 Depto. de Ciências Atmosféricas-IAG, Universidade de São Paulo, São Paulo. E-mail: pscheidt@model.iag.usp.br.

2 Depto. de Física, Universidade Federal do Paraná, Cx Postal 19044, 81531-990 Curitiba, Brazil. E-mail: grimm@fisica.ufpr.br

The precipitation station data are averaged in  $1^{\circ} \times 1^{\circ}$  latitude/longitude boxes. In each box the running 3-day precipitation totals are computed and the values are attributed to the central days. Gamma distributions are fitted to the 51 values of these accumulated precipitations for each day of November and July in the period 1950-2000, and each value is replaced by its correspondent percentile. Extreme events correspond to percentiles equal or above 85.

The average number of extreme events in November (0) and July (+) is computed for each box and three categories of years: EN, LN and neutral. The EN and LN years are the same as in Grimm (2003, 2004). These averages include at least 9 EN years, 8 LN years and 18 neutral years. The analyzed period encompasses 13 EN, 12 LN and 26 neutral years. The differences between these averages for EN and neutral years as well as for LN and neutral years, and their statistical significance, are displayed on maps.

In these maps, there are "homogeneous areas" in which the number of extreme events increases significantly during EN years and/or decreases during LN years. For the extreme events in these areas we analyzed the associated atmospheric conditions during EN, LN and neutral years.

Series of average daily rainfall are computed for each of these areas, and the extreme events are determined, after following the same procedures as described above for the  $1^{\circ} \times 1^{\circ}$  boxes. The atmospheric conditions associated with the extreme events during the three categories of years were analyzed through Principal Component Analysis (PCA) and composites.

The T-mode PCA (as in Salles and Compagnucci 1997) of geopotential height at 850 e 250 hPa during extreme events in EN, LN, and neutral years discloses the most recurrent atmospheric patterns during these events in each category.

Finally, anomaly composites of precipitation, geopotential height, sea level pressure, moisture flux and its divergence for extreme events in each category are compared with monthly anomalies for EN and LN events, in order to understand the change of frequency of the extreme events. Composites of these variables were also computed separately for EN years with less and more extreme events than neutral years, to verify the differences between these two EN categories.

For each homogeneous area the mean monthly precipitation series and the number of extreme events

are correlated with SST. Correlations using only EN or LN years were also computed to assess inter-event variations.

### 3. RESULTS

There are three homogeneous regions (A, B, C) in southern Brazil in which extreme precipitation events increase significantly during November (0) of EN years and one larger region (D) in which these events are reduced during LN years. In July (+) of EN episodes there is significant increase of extreme events in one region (E) (Fig. 1).

The correlation coefficient patterns of SST with the number of extreme events and SST with average precipitation in each of those homogeneous areas are similar to the SST anomalies associated with ENSO episodes, showing that they really impact not only on the monthly precipitation but also on the number of extreme events (Figs. 2 and 3). For areas A and B these correlation patterns, as well as the atmospheric patterns associated with extreme events, are very similar to those for area D, which is expected, for area D contains areas B and C. Therefore, further analyses for November will concentrate on area D and the coastal area A.

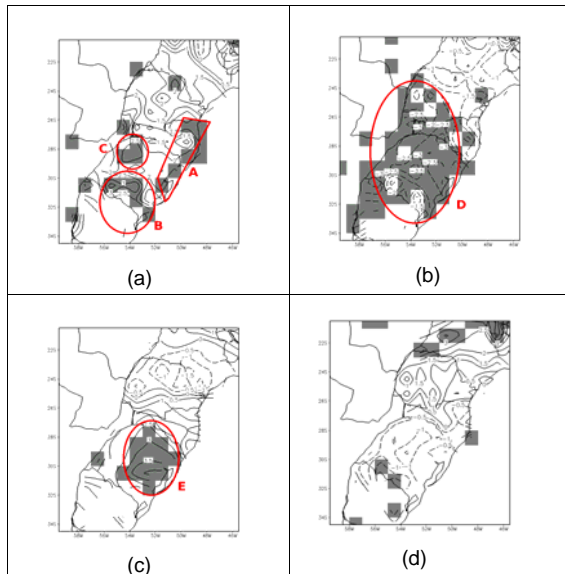


**Figure 1:** Difference between the mean number of extreme events during November (0) of (a) EN and neutral years, (b) LN and neutral years. Difference between the mean number of extreme events during July (+) of (c) EN and neutral years, (d) LN and neutral years. Shaded areas indicate significant difference with confidence level better than 90%. Red contours indicate homogeneous areas.

Significant positive correlation between November SST and average precipitation in area A is found in tropical central-east Pacific Ocean, in the Indian Ocean and subtropical South Atlantic (Fig. 2a). Negative significant values are concentrated in the subtropical south Pacific and western equatorial Pacific. The correlation patterns of SST with frequency of extreme

events are similar, except for the negative values in northern Pacific and the eastward shift of the highest correlation coefficients in equatorial Pacific (Fig. 2b).

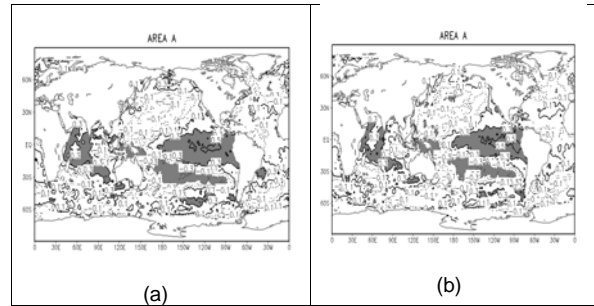


**Figure 2:** Correlation coefficients between November SST and (a) average monthly precipitation and (b) number of extreme events in area A. Shaded regions indicate significant correlation with confidence level better than 95%.

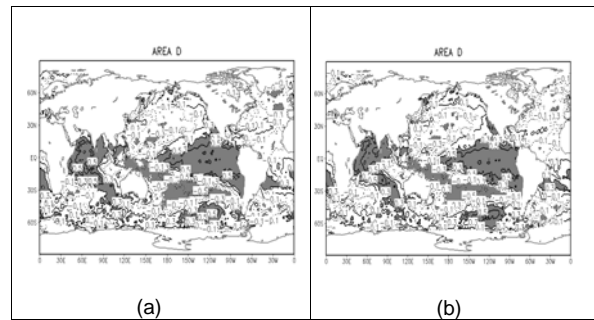


**Figure 3:** Correlation coefficients between November SST and (a) average monthly precipitation and (b) number of extreme events in area D. Shaded regions indicate significant correlation with confidence level better than 95%.

The correlation of SST with November precipitation and SST with frequency of extreme events in area D is significant over a broader region than for area A in the tropical eastern Pacific, from the west coast of North America to the subtropical west coast of South America (Fig. 3a, b). Both correlation maps are very similar.

We also calculated the correlation coefficients using only EN years. Then the significant values indicate regions in which inter-event variation of SST anomalies is responsible for inter-event variation of precipitation and number of extreme events. Such correlation maps for area D (not shown) indicate that variations of SST in equatorial eastern Pacific are important in determining the observed anomalies during the EN episodes.

The correlation between July SST and precipitation or between SST and frequency of extreme events in area E shows that excessive rainfall or more frequent extreme events in July (+) of EN years is associated with positive SST anomalies in the southern tropics and extratropics of the eastern Pacific, as well as in the Indian Ocean and the subtropical South Atlantic. Significant correlations are also present in northern Atlantic and Pacific, suggesting a possible role of interdecadal variability, which has significant signature in these regions (Figs. 4a, b). Both correlation maps are very similar.

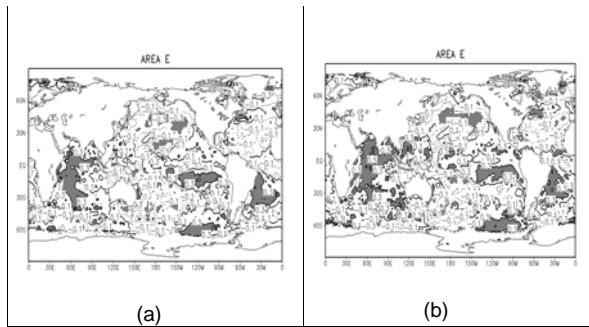


**Figure 4:** Correlation coefficients between July SST and (a) average monthly precipitation and (b) number of extreme events in area E. Shaded regions indicate significant correlation with confidence level better than 95%.

The T-mode Principal Component Analysis (T-PCA) of geopotential height at 850 and 250 hPa during extreme precipitation events in each homogeneous area (A, D, and E) and each category of year (EN, LN, and neutral) shows that for extreme events in a given area the most recurrent patterns are basically the same in the three categories of years, especially near the focused area. The similarity is greater for extreme events in EN and neutral years.

At low-level (850 hPa), the first modes in each category of year for extreme events in areas A and D during November (0) feature zonal flow at mid-latitudes and high pressure centers in the subtropics of Atlantic and Pacific Oceans with a relative low pressure over the continent (Fig. 5a). For extreme events in area E during July (+) of EN episodes the Atlantic high extends over the continent and the relative low is weaker, with little northward penetration (Fig. 5b). In both cases the temporal series of factor loadings has negative values.

The other modes (not shown) in each category show different patterns with geopotential anomaly centers in mid-latitudes that generally favor the intrusion

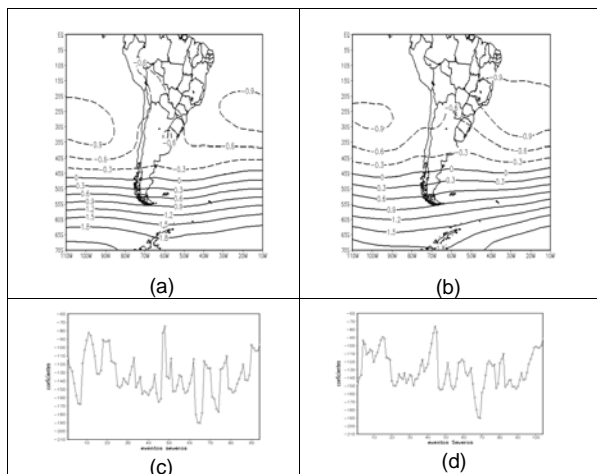


**Figure 5:** First principal component of the T-PCA of geopotential height at 850 hPa during extreme precipitation events on (a) November (0), and (b) July (+) of EN years in areas A and E, respectively. The factor loading series are shown in (c) and (d).

of cold air masses from higher latitudes.

At 250 hPa there is a cyclone-anticyclone pair over the subtropics of South America that intensifies the subtropical jet. For extreme events during July (+) in area E the first modes show a weaker zonal flow than for extreme events during November (0) in area D. The higher order modes feature tripoles in mid-latitudes, with one center over the continent and opposite centers over the adjacent oceans.

Composites of monthly anomalies of some atmospheric parameters during November (0) and July (+) of EN and LN years show that during EN years these anomalies are much more alike the anomalies observed during extreme precipitation events in the homogeneous areas than monthly anomalies during LN years (see, for example, Fig. 6). Therefore, atmospheric perturbations produced by EN episodes are favorable to the occurrence of extreme events, which explains their higher frequency during EN episodes.

Composites of geopotential height anomalies at 850 hPa for extreme precipitation events in area A during November (0) of EN years show that there is lower pressure over the southern part of the continent and higher pressure over the southwestern Atlantic (Fig. 6a). The high pressure anomaly that consistently appears during November (0) of EN years southwest of SA (Fig. 6c) is shifted toward the southern Atlantic during extreme events in the coastal area A (compare Figs. 6a and 6c).

At higher levels the similarity between the anomalies present during extreme events and those monthly anomalies associated with EN episodes is even greater (not shown).

High precipitation in extreme rainfall events in coastal area A during November of EN years is favored by anomalous convergence of moisture flux from the continent and the Atlantic Ocean (Fig. 7a, c), mainly associated with low-level anomalous circulation (Fig. 6a). During extreme events of LN years the low pressure that on the average dominates southeastern South America in these years (Fig. 6d) is extended southward (Fig. 6b). Over mid-latitudes of the Pacific and Atlantic oceans there are dipoles of opposite polarity. The Atlantic subtropical high and the low pressure over southeastern/southern Brazil intensify the moisture inflow from the Atlantic into area A (Fig. 6b and 7d). Contrary to EN years, there is no moisture flux from the continent into area A. The moisture fluxes anomalies are similar to the monthly anomalies.

Extreme events in area D during November of EN events are associated with low pressure over the southern part of the continent that extends over the Atlantic, and a high pressure center south of SA that directs extratropical systems into SA (Figure not shown). These patterns are also present in the monthly anomalies during EN episodes. This explains the higher frequency of extreme events. The moisture flux from central SA into the area is very intense, as well as its convergence. Extreme events in LN years are associated with atmospheric patterns similar to those associated with extreme events in EN years. They are fairly different from the monthly anomalies associated with LN episodes. Therefore the frequency of extreme events during LN episodes is much lower.

Composites for extreme events in July (+) of EN years show basically patterns similar to the average monthly anomaly patterns with intensified magnitude, with the low pressure in the west part of SA shifted over area E. During LN years circulation patterns associated with extremes are similar (Figures not shown).

Over the period analyzed there are EN episodes in which the number of extreme events is less than normal while in most of the episodes it is above-normal. The atmospheric conditions during these two categories of episodes were compared.

During EN episodes with more extreme events the sea level pressure anomaly dipole in the eastern Pacific, with subtropical low pressure extending over the continent and extratropical high pressure center southwest of SA is close to the continent and significant (Fig. 8a). Yet during EN episodes with less than normal extreme events this anomaly dipole is weaker and shifted westward, toward central Pacific (Fig. 8b). The same kind of difference is noted with respect to EN episodes with above or below normal number of extreme events in area D (Figs. 8c and 8d). The shift of that pattern is probably related with the magnitude and shift of SST anomalies. SST anomalies are strongest and more extensive during EN episodes with higher frequency of extreme events in both area A and D (Figure not shown).

There are not significant differences concerning moisture divergence in area A for EN with opposite impact on the number of extreme events (Figs. 9a, b), but the anomalous moisture flux from northern SA toward area A are significant only in those EN episodes with higher number of extreme events (Figs. 9c, d). On the other hand the anomalous moisture convergence into area D is only significant when the number of extreme events is above-normal, as well as the moisture flux.

EN episodes in which there are less than normal extreme events during July (+) in area E are characterized by lack of late SST anomalies in eastern Pacific and by higher low-level pressure over this area (Figures not shown).

#### 4. CONCLUSIONS

There are extensive areas in Southern Brazil in which the frequency of extreme precipitation events increases significantly during November (0) of EN years and decreases during LN years. There is also an area where number of extreme events increases during July (+) of EN years.

We analyze the atmospheric conditions associated with extreme events in November (0) in two of these areas: one is very extensive and reaches inland, to the boundaries with Argentina and Paraguay (D), while the other is a narrow coastal area (A). Although there are some similarities between the

anomalous fields associated with extreme events in these areas, there are also noticeable differences.

The relationships between SST and monthly rainfall and between SST and frequency of extreme events are generally alike for a given region, indicating that monthly total precipitation and extreme events are related with similar SST conditions. For area A, however, the frequency of extreme events has stronger correlation with SST temperatures in equatorial eastern Pacific than has monthly rainfall.

When calculating correlation coefficients between SST and precipitation or between SST and frequency of extreme events only for EN years or LN years, the patterns show regions in which inter-event SST differences have the greatest impact on the ENSO-related precipitation anomalies. The greater differences appear for November in the equatorial eastern Pacific.

According to the T-PCAs of geopotential height at lower and upper levels during extreme precipitation events, the most recurrent patterns are basically the same for all categories of year. At high levels there is a slightly undulating zonal flow, with a trough over western SA in the subtropics. At lower levels, there are subtropical highs over the Atlantic and the Pacific, and a low over southwestern SA, which favors warm and humid air flow from northern SA into southeastern SA.

The highest-order T-modes feature patterns that appear during some of the extreme events and determine the inter-event variations.

The most frequent of these patterns appear in the anomaly composites for atmospheric conditions during extreme events. These composites have many similarities with the monthly mean perturbations produced by EN episodes. Therefore, the higher frequency of extreme events during EN years is due to favorable conditions, that is to say, the patterns associated with extreme events are present most of the time during these episodes, being caused by large-scale remote forcing. During LN years the monthly mean perturbations are generally opposite to the patterns associated with extreme events. Therefore, conditions are unfavorable for them to appear and their frequency is reduced. The occurrence of an extreme event during LN years in those areas demands that the usual LN anomaly patterns be weakened and/or shifted. Once a system is strong enough to intrude in such unfavorable conditions it usually produces strong precipitation. Therefore, although the extreme events during LN are rare, they are intense.

*Acknowledgments.* This work was supported by the Conselho Nacional de Desenvolvimento Científico e Tecnológico (CNPq, Brazil) and the Interamerican Institute for Global Change Research (IAI-CRN 055). The first author is supported by a fellowship from CAPES (Brazil).

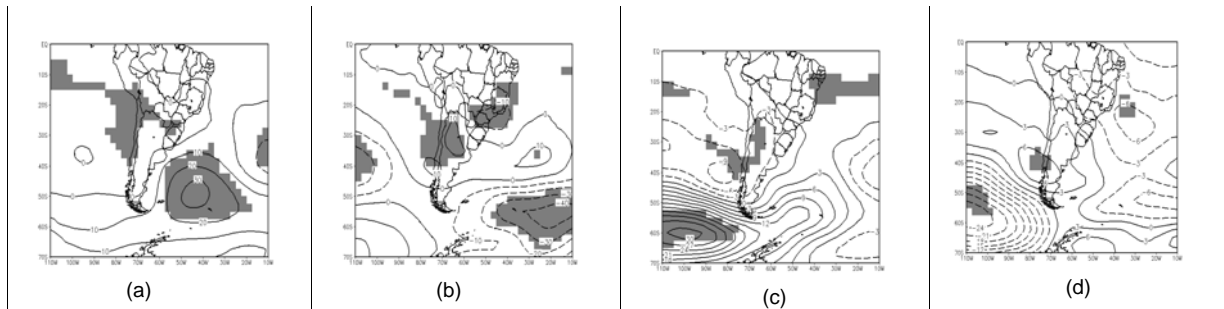


**Figure 6:** Composites of geopotential height anomalies at 850 hPa for extreme precipitation events in área A during November of (a) EN years and (b) LN years. Figures (c) and (d) show composites of monthly anomalies in November of EN and LN years respectively.

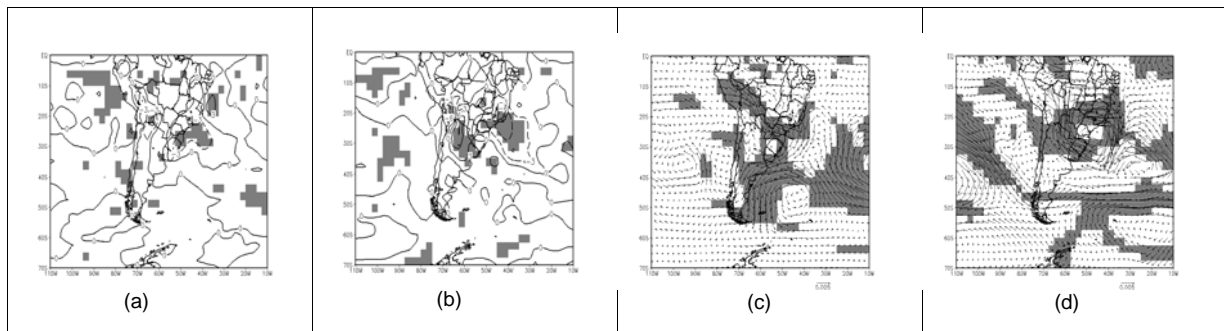


**Figure 7:** Composites of vertically integrated moisture divergence anomalies ( $\times 10^{-11} \text{ m}^{-1}$ ) for extreme precipitation events in área A during November of (a) EN years and (b) LN years. Figures (c) e (d) show composites of the moisture flux anomalies during the same periods.

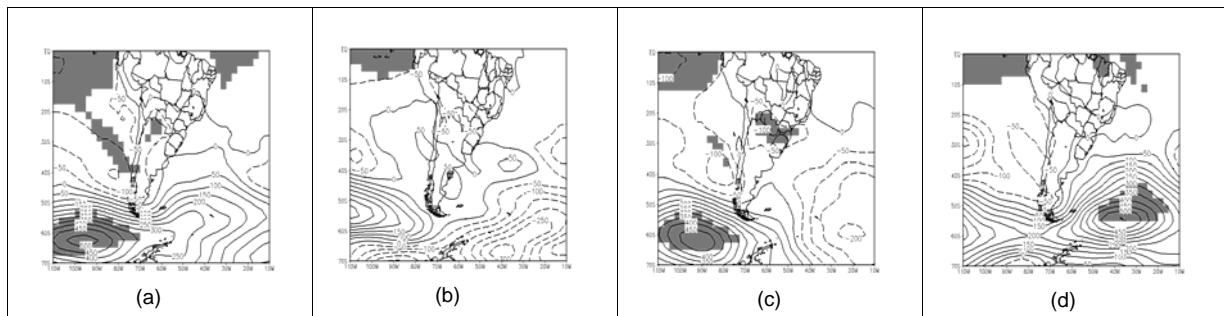


**Figure 8:** Composites of sea level pressure monthly anomalies for November (0) of EN years with (a) more and (b) less than normal extreme rainfall events in area A. Figures (c) e (d) show the composites for area D.

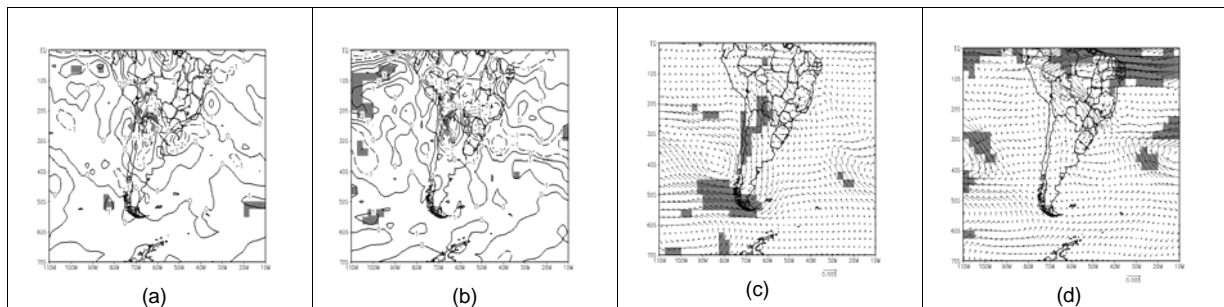


**Figure 9:** Composites of moisture divergence monthly anomalies ( $\times 10^{-9} \text{ m}^{-1}$ ) for November (0) of EN years with (a) more and (b) less than normal extreme rainfall events in area A. Figures (c) e (d) show the composites of moisture flux anomalies for the same situations.

## REFERENCES

- Barros, V.R. and G.E. Silvestri, 2002: The Relation between Sea Surface Temperature at the Subtropical South-Central Pacific and Precipitation in Southeastern South America, *J. Climate*, **15**, 251-267.
- Compagnucci, R.H and M.A.Salles, 1997: Surface Pressure Patterns during the Year over Southern South America, *Journal of Climatology*, **17**, 635-653.
- Diaz, Alvaro F., Caarem D. Studzinski and Carlos R. Mechoso, 1998: Relationships between Precipitation Anomalies in Uruguay and Southern Brazil and Sea Surface Temperature in the Pacific and Atlantic Oceans. *J. Climate*, **11**, 251-271.
- Enfield, David B. and Alberto M. Mestas-Nunez, 1999: Multiscale Variabilities in Global Sea Surface Temperatures and their Relationships with Tropospheric Climate Patterns. *J. Climate*, **12**, 2719-2733.
- Grimm, A. M., S.E.T. Ferraz and J. Gomes, 1998: Precipitation anomalies in Southern Brazil associated with El Niño and La Niña events. *J. Climate*, **11**, 2863-2880.
- Grimm, A. M., M. E. Doyle and V. R. Barros, 2000: Climate variability in Southern South America associated with El Niño and La Niña events. *J. Climate*, **13**, 35-58.
- Grimm, A. M., 2003: The El Niño impact on the summer monsoon in Brazil: regional processes versus remote influences. *J. Climate*, **16**, 263-280.
- Grimm, A. M., 2004: How do La Niña events disturb the summer monsoon system in Brazil? *Climate Dynamics*, **22**, 123-138.
- Kidson, J. W., 1975: Tropical eigenvector analysis and the Southern Oscillation. *Mon. Wea. Rev.*, **103**, 187-196.
- Kousky, V.E., I.F.A. Cavalcanti and M.T. Kayano, 1984: review of the Southern Oscillation: oceanic-atmospheric circulation changes and related rainfall anomalies. *Tellus*, **36A**, 490-504.
- Mason S. J., and L. Goddard, 2001: Probabilistic Precipitation Anomalies Associated with ENOS. *Bulletin of the American Meteorological Society*, **82**, 619-628.
- Mestas-Nunez, Alberto M. and David B. Enfield, 2001: Eastern Equatorial Pacific SST Variability: ENOS and Non-ENOS Components and their Climatic Associations. *J. Climate*, **14**, 391-402.
- Rayner, N. A., D. E. Parker, E. B. Horton, C. K. Folland, L. V. Alexander, D. P. Rowell, E. C. Kent, A. Kaplan (2003), Global analyses of sea surface temperature, sea ice, and night marine air temperature since the late nineteenth century, *J Geophys Res* 108 (D14): 4407, DOI 10.1029/2002JD002670.
- Souza, E. B. and T. Ambrizzi, 2002: ENOS impacts on the South American rainfall during 1980s: Hadley and Walker circulation. *Atmósfera*, **15**, 105-120.